Emergent Materials
https://doi.org/10.1007/s42247-024-00751-9

ORIGINAL ARTICLE

Proof of concept study for radial compression strength & shape memory effect of 3D printed double arrowhead PLA stent

Ayushi Thakur[1] · **Umesh Kumar Vates**[2] · **Sanjay Mishra**[3]

Received: 20 March 2024 / Accepted: 22 May 2024

Abstract
Self-expanding biodegradable stents are expected to replace metallic stents in the treatment of peripheral artery disease, which may cause numerous problems to human health. Since the materials used in polymeric-based stents are more suited to human cells, they are considered the next generation of these medical devices. The fabrication of polymeric stents with optimized parametric 3D printing settings can surely improve their mechanical performance including radial strength which is considered as one of the crucial factors for the efficient functioning of the stent. The radial supporting capability of the stent should be taken into consideration by the vessel to restore the patency of blocked peripheral arteries with varying characteristics and functions. In this work, a double arrowhead 3D-printed PLA stent's distinct mechanical properties are developed and described. The fused deposition modeling mechanism of 3D printing was used to manufacture the double arrowhead stent specimens to analyze the radial strength. For the analysis of Stents with different sets of geometric parameters (outer diameter, height of stent, strut diameters, width of strut) were developed. The results demonstrate that for the same set of other dimensional parameters, the lowest diameter stents showed the highest radial strength in the experiments also it is evident that when strut diameter increases along with the angle between the axial direction and support strut (ϕ), and the angle between the axial direction and re-entrant strut (θ), results increase in the support strut cross-sectional (coverage) area resulting in the increased radial strength. Another observation is that the radial recovery ratio and length recovery ratios are 91 to 95% and 92 to 98% respectively which is suitable for polymeric stent application.

Keywords Bioabsorbable stent · 3D Printing · Polylactic acid · Radial strength

1 Introduction

Coronary arteries disease occurs when plaque builds up on the inner part of the arteries and it blocks the way of flowing blood into them. The consequences of this build-up plaque result in the narrowing of the passage and completely blocking the passages at the advanced stage of the decrease. Coronary artery stenting is the best solution to treat this life-threatening disease. The radial force produced by stents stops the vessel wall's elastic recoil. Radial strength has traditionally been the main feature of stent designs to resist the vascular bed's compressive forces and prevent the artery from abruptly recoiling [1]. The fourth revolution in coronary innovation has been named biodegradable vascular stents [2]. BVS restores the damaged blood vessels temporarily before progressively disintegrating to leave behind a thin, naturally occurring layer of cells inside the artery [3]. refer to Fig. 1. This removes the major side effects of long-term metallic stent use, including revascularization of advanced target lesions, vasomotor dysfunction, and late in-stent restenosis [4–6]. Biodegradable polymer stents (BPS) have gained attention recently due to their improved biocompatibility, biodegradability, and processability [7, 8]. However, polymers have inferior mechanical properties

✉ Ayushi Thakur
thakur.ayushi@gmail.com

Umesh Kumar Vates
ukvates@amity.edu

Sanjay Mishra
smme@mmmut.ac.in

[1] Department of Mechanical Engineering, Ayushi Thakur, Amity University Uttar Pradesh, Noida, India

[2] Department of Mechanical Engineering, Dr. Umesh Kumar Vates, Amity University Uttar Pradesh, Noida, India

[3] Department of Mechanical Engineering, Dr. Sanjay Mishra, Madan Mohan Malaviya University of Technology, Gorakhpur, India

Published online: 10 June 2024

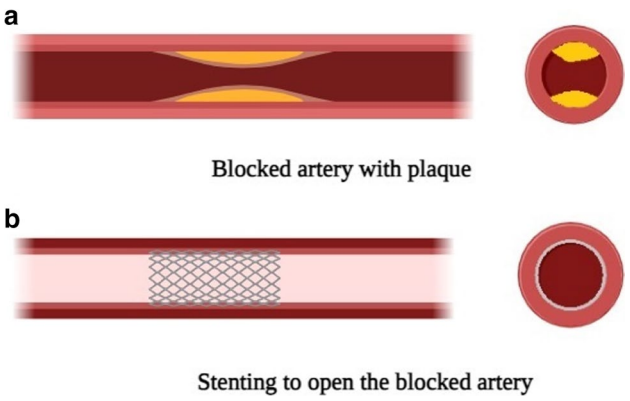

Fig. 1 **a** A diagrammatical representation of a blocked artery from plaque **b** Stenting to open the blocked artery

to metals, the resulting polymer stents typically have weak radial strength and radial recoil [9]. Based on this fact, the main problem facing the stent-making businesses is how to enhance the mechanical qualities of the BPSs. Researchers, academicians, and medical experts have suggested various suggestions based on their research work and observations. Modification of the build materials has been explored based on mechanical strength [10, 11]. Major influencing factors for the efficient performance of a BPS are stent material and its mechanical properties, stent structure, stent dimensions, strut thickness, and manufacturing processes involved in the formation of stents. One of the main factors influencing the mechanical behavior of the stent is its structure and associated geometry. For biodegradable polymeric stents, the mechanical parameters include axial foreshortening, radial recoil, radial strength (force), and flexibility [12]. Refer to Fig. 2. Struct thickness has also been considered to alter the mechanical properties of any BPS as struct thickness can improve the radial force [13, 14].

Biodegradable and renewable, polylactic acid (PLA) is one of the biopolymers present in compostable thermoplastics [15]. PLA also comes under the class of stimuli-triggered materials which change their configuration in the

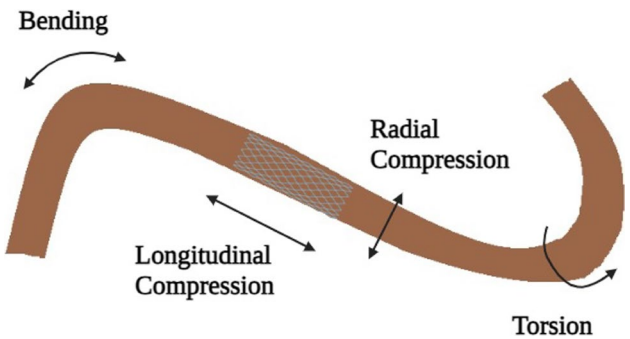

Fig. 2 Aspects of the mechanical properties of the stent: bending, radial compression, longitudinal compression, and torsion

presence of external stimuli (temperature) [16–18]. PLA's shape memory effect is a result of the polymer's morphology and structure, which are made up of two different domain sets: amorphous domains that function as the reversible phase and crystalline domains that act as the fixed phase. PLA offers a wide range of application possibilities in many biomedical fields, such as vascular stent, surgical sutures, drug release, thrombus removal, and scaffolds for tissue engineering, because of its superior mechanical ability, Shape Memory Effect, and biocompatibility [19, 20]. It has been noted that 3-dimensional (3D) printing, or additive manufacturing, has developed into a flexible technology and affordable option for customized fabrication for biomedical applications. The emergence of 4D printing, which involves gradual alterations in form, characteristics, or functions due to external stimuli, is a result of 3D printing and is widely being used to fabricate metallic and polymeric stents used for blocked arteries and biomimetic intestinal applications [21, 22].

In the following paragraph, there is a summary of a few of the notable findings. Lin, C. et [23] generated two types of personalized shape memory vascular stents using 4D printing that had structures with a negative Poisson's ratio and in their research structure was optimized using a genetic algorithm. To investigate the mechanical characteristics of the stents, three-point bending, radial compression, and axial compression tests are performed. Additionally, the stent's shape memory properties were examined in vitro feasibility testing, which showed that it exhibited good shape memory behaviors and that NPR structures are a great option for treating vascular stenosis. Wu et al. [24] utilized PLA filaments with fused deposition modeling printers to fabricate stents with a negative Poisson's ratio (NPR) structure. Subsequently, they examined the PLA stent's radial compressive characteristic; however, despite the positive results of these investigations, the stent's design remains problematic. Ana M. Sousa et al. [25] proved that increasing plastic deformation caused by a reduction in strut thickness of a PLA stent lowers the radial recoil ratio and raises the absolute magnitude of foreshortening.

In this experimental work, double arrowhead auxetic PLA stent specimens were made by 3D printing using the fused deposition modeling method to assess the radial strength and Shape memory effect of the structure. However, no comprehensive examination of the biocompatibility and biodegradation of the suggested stent was conducted. Polymeric stents on the optimized printing settings have been designed with a double arrowhead auxetic structure as shown in Fig. 3. Auxetic structures have a negative Poisson's ratio, meaning that they expand laterally when they are stretched horizontally. Figure 3 presents this idea in great detail. The impact of stent diameter, strut diameter, and other geometrical variables of a set of stents on radial strength and shape memory

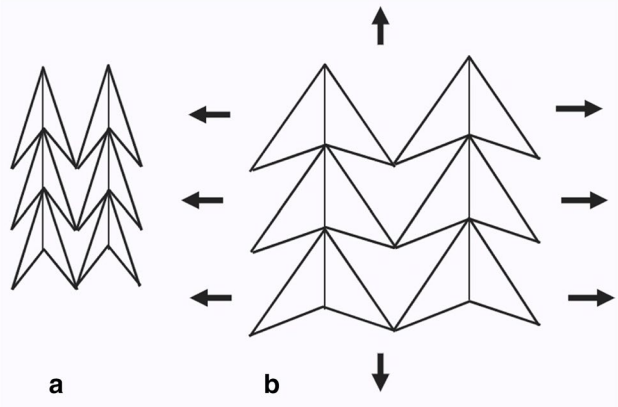

Fig. 3 Two-Dimensional double arrow topological structure (**a**) before stretching (**b**) after stretching

effect were analyzed. Measurements of change in diameter and length were also carried out for diameter recovery and length recovery ratio.

2 Materials & methods

2.1 Design of double arrowhead Auxetic structured PLA stent

The majority of the vascular stent models studied in the relevant studies conducted recently have somewhat basic structures, like spiral, corrugated, and Z-shaped architectures. A double arrowhead stent may simultaneously reduce the stent's radial and longitudinal sizes during expansion and crimping, such test stents were fabricated using optimized 3D printing parameters settings on the fused deposition modeling method. The ability to expand in the longitudinal and radial direction of such structure allows good anchorage with arterial walls [26, 27]. Auxetic-designed stents feature special deformation properties that lead to improved mechanical properties including foreshortening, radial strength, and radial recoil [23, 28]. The stent's structural unit in this work was created using the Autodesk Fusion 360 design program and is depicted in Fig. 4. The three-dimensional representation of the stent is created by repeating the arrowhead structural unit around its circumference and along its axis. Table 1. presents size parameters that can be used to establish the shape of the 3D-printed stent specimen.

2.2 Experimental setup and materials

In this research project polylactic acid filament was acquired from Numakers India. The filament's dimensions are 1.75 ± 0.03 mm in diameter, 1.24 g cm-3 in density, and 55 °C for the glass transition temperature. The PLA filament has a modulus of 2315 MPa and a tensile strength of 50 MPa. To test the radial strength of the double arrowhead auxetic 3D printed stent structure, The 10 T (HUD-B612-S) universal testing apparatus, equipped with a 10kN load cell, manually hardened jaws, and specially designed compression platens, was used for the experiment. Using this apparatus longitudinal compression on the cylindrical part (cylindrical stent) can be measured. A set of experiments were performed on the machine for each specimen. Another aspect of testing is to analyze the radial strength through the crimping device, for that purpose, a stent crimping device ZwickRoell compression testing machine was used, the analysis involves measurement of crimped dimensions to calculate the percentage change in longitudinal and radial dimensions of each specimen of the sets.

2.3 3D printing of Stent structure

The standard stent design features examined in the pertinent literature served as a guide for creating a set of stents'

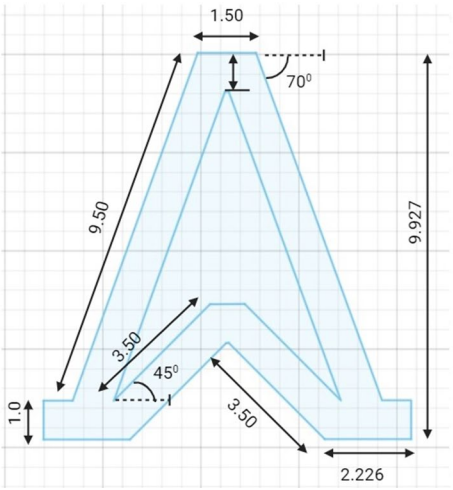

Notations	Dimensions
L	9.5mm
m	3.5mm
h	9.927mm
t	1mm
d	1.5mm
ϕ	20^0
θ	45^0
D	12mm
H	39.70mm
T	1.2mm

Fig. 4 CAD Drawing of Double Arrowhead PLA Structure unit

Table 1 Geometrical parameters of 3D printed stent specimen

S. No	Notation	Description
1	L	Strut length
2	T	the stent strut thickness of the stent
3	M	Re-entrant strut length
4	H	The height of the unit
5	D	Link width
6	T	Strut width
7	Φ	The angle between the support strut in the axial direction
8	Θ	angle between the re-entrant strut and the axial direction
9	D	The outer diameter of the stent;
10	H	total length of the stent;

geometries [29–31]. The stent specimens are created in the experimental analysis using a fused deposition modeling mechanism (Fig. 5). The following variables are needed for the FDM process: layer thickness, printing speed, raster angles, build orientation, nozzle temperature, and bed temperature. The optimal values of parameters for printing PLA specimen stents are obtained from the experimental findings [32]. The chosen printing parameters—nozzle temperature, printing speed, and layer thickness have shown to be important determinants of mechanical qualities like tensile, flexible strength, and radial strength. The 3D design tool Autodesk Fusion 360 was used to create the sample for this investigation. This file configuration is converted to a Standard Tessellation Language file format that is suitable for 3D printing. This is further converted into a slice of the CAD model into layers for deposition using ULTIMATE CURA software. The test specimen is created using a Polymeric 3D printer called CREALITY ENDER 3, which is based on fused deposition modeling. Despite the specific input parameter values, this polymer feed-based 3D printer can manufacture many test specimens. This 3D printer's versatility in adjusting the input parameter setting was not its only drawback. To get the solid-like structure of the specimen, the infill value was set to 100%. Table 2 lists the primary optimized printing parameters. Using Ultimate Cura Software, the 3D model was sliced into several layers; Table 3 displays the many groups of stent specimens manufactured using various input geometric configurations, While groups B, D, and E have the same strut sizes (T = 1.5 mm), groups A, B, and C have distinct strut diameters (1.2 mm, 1.5 mm, and 1.8 mm).

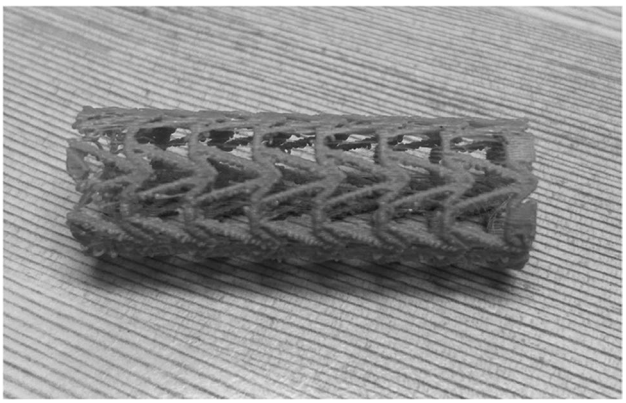

Fig. 5 3D printed double arrowhead PLA stent

2.4 Mechanism for testing radial strength

One of the main characteristics that keep the stent from recoiling is its radial strength, which supports the cylindrical shape structurally and is an essential mechanical characteristic to check for in a bioabsorbable polymeric stent. The Radial loading test is the most admitted method to evaluate the stent's mechanical properties. To measure the radial force, two techniques are used in this research: The compression test, which involves inserting a stent between two parallel plates and measuring the resistance force it experiences when compressed, and the crimping test to analyze the radial compression.

2.4.1 Compression experiment for PLA stent:

A Zowikroell electromechanical tabletop testing machine, an electronic universal testing device controlled by a microcomputer, was used to test the compression experiment refer to Fig. 6. The PLA stent was positioned along x-axis on the platform, and until the stent was crushed, the pressure plate was compressed at a rate of one millimeter per minute. When applying the compressive force, the stent's radial direction—which was perpendicular to its axis—was followed. The radial force against the platen's displacement was measured during the compression operation.The whole stent length was split to normalize the radial force, making it easier to compare stents with various lengths and geometric features. The radial force of the stent material (per unit length) F (N/mm) was calculated as a function of radial displacement (mm).

Table 2 Optimized parameters for printing the specimen [32]

S. No	Parameters	Code	Optimized Values
1	Layer Thickness (mm)	LT	0.23 mm
2	Nozzle Temperature (°C)	NT	208 °C
3	Printing Speed mm sec^{-1}	S	55.5 mm sec^{-1}

Table 3 Geometric characteristics and experimental groups of PLA stent specimens manufactured by 3D printing. Stent thicknesses differ in A, B, and C. In contrast, Groups B, C, and D exhibit the same stent thickness (T)

Set	Number	D(mm)	H(mm)	T(mm)	L(mm)	m(mm)	t(mm)	d(mm)	ϕ/ ◦	θ/ ◦
A	A1	12	39.70	1.2	9.5	3.5	1	1.5	20	45
	A2	14	39.70	1.2	9.5	3.5	1	1.5	20	45
	A3	16	39.70	1.2	9.5	3.5	1	1.5	20	45
B	B1	12	39.70	1.5	9.5	3.50	1	1.5	25	45
	B2	14	39.70	1.5	9.5	3.50	1	1.5	25	45
	B3	16	39.70	1.5	9.5	3.50	1	1.5	25	45
C	C1	12	39.70	1.8	9.5	3.5	1	1.5	25	45
	C2	14	39.70	1.8	9.5	3.5	1	1.5	25	45
	C3	16	39.70	1.8	9.5	3.5	1	1.5	25	45
D	D1	12	41.10	1.5	7.5	2.75	1	1.5	30	55
	D2	14	41.10	1.5	7.5	2.75	1	1.5	30	55
	D3	16	41.10	1.5	7.5	2.75	1	1.5	30	55
E	E1	12	41.10	1.5	6.5	2.5	1	1.5	30	65
	E2	14	41.10	1.5	6.5	2.5	1	1.5	30	65
	E3	16	41.10	1.5	6.5	2.5	1	1.5	30	65

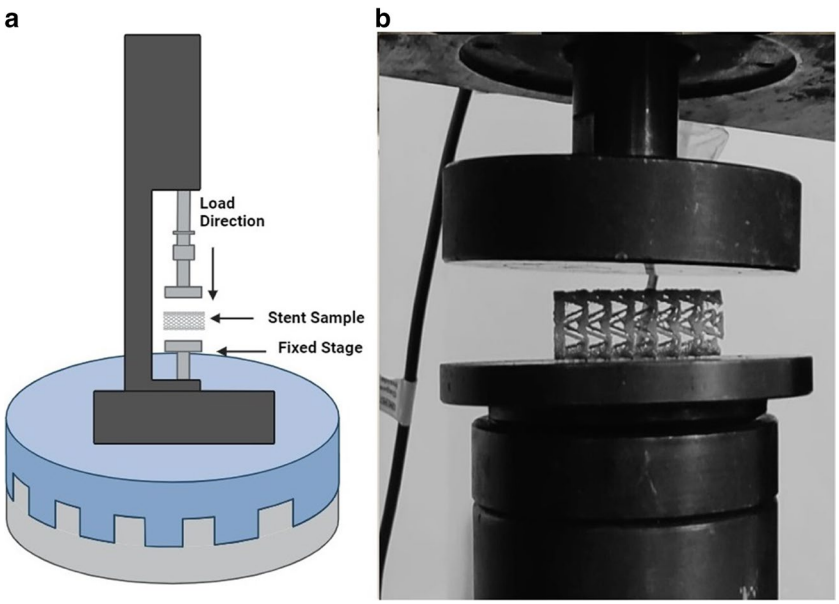

Fig. 6 **a** Compression experiment of PLA stent. **b** Radial compression test on universal testing machine

2.4.2 SME experiment for PLA stents

ZwickRoell compression testing equipment was utilized to conduct a proof-of-concept investigation on a 3D-printed PLA stent with an auxetic construction by SMEs and crimping devices refer to Fig. 7. The diameter recovery ratio and length recovery ratio were computed by calculating the range of the stent's diameter and length following deformation and recovery. The PLA stent's initial diameter (Di) and initial length (Hi) were measured before to the experiment. There are three steps in the Shape memory experiment. The stent's distortion, which produced the crimped shape, was the initial step. The circumferential structural components of the PLA stent were deformed and close to one another after the crimping process was stopped and the diameter of the stent was moderately lowered. The crimped stent has come to a stop and is fixed at room temperature in the second step of the procedure. After being firmly fixed, the crimped stent was gently removed from the crimping machine. The PLA stent's crimped length HC and crimped diameter DC were measured. The third and last step of the procedure is the stent recovery, which restores the original stent through recovery. After that, the squeezed PLA stent was immersed in the water bath, with the water temperature for PLA stent recovery set at 65^0 C, until its shape remained unchanged. Measurements were made on the recovery length (Hr) and

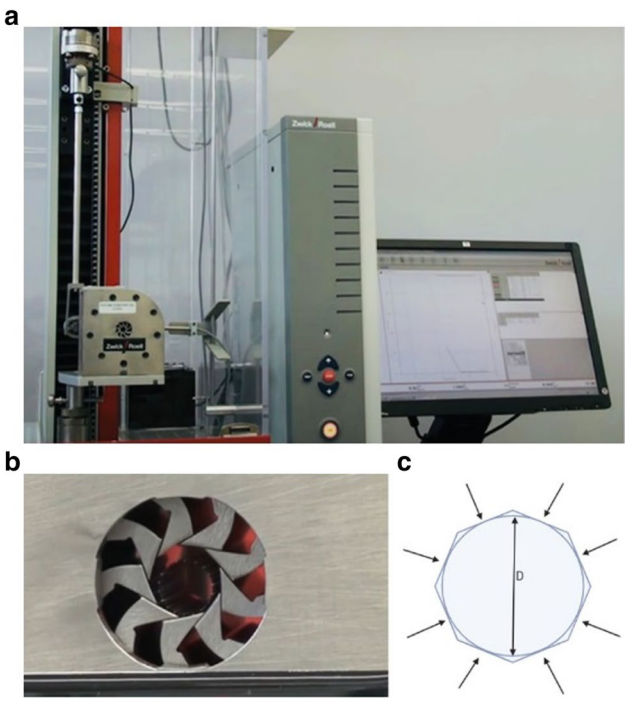

Fig. 7 **a** Experimental setup for the measurement of radial force using a crimping machine. **b** Radial Force testing apparatus **c** simulated 8 rigid crimper plates

recovery diameter (Dr). Formulas (1) and (2) were used to calculate the diameter recovery ratio and length recovery ratio of the 3D-printed PLA stent.

$$R_D = D_r/D_i \quad (1)$$

$$R_H = H_r/H_i \quad (2)$$

R_D and R_H depict the diametral recovery ratio and length recovery ratio for 3D-printed PLA stents. Whereas D_i Initial Diameter, H_i Initial Length, Dc Crimped Diameter, Hc Crimped Length, Dr Recovery Diameter, Hr Recovery Length.

3 Results & observations

3.1 Compression experiment result

a) **When the stent strut thickness (wall thickness) is different (Considering Group A, B, and C)**

Every 3D-printed PLA stent specimen was used for the compression experiment; the experimental observations are displayed in Fig. 8 as a plot between compression force and displacement. Each group has three PLA stent diameters but the same stent thickness and auxetic structural geometric characteristics. At the beginning of the curves, the stents' radial distortion gradually grew with comparatively big slopes. The compressive characteristics of the 3D-printed PLA stents in each group with distinct diameters vary relatively little. However, the curves gradually flattened out as the compressive force rose, and the influence of different stent diameters on radial force grew additionally important. It has been observed that the vascular stent primarily exhibited elastic deformation at minimal radial displacement. When the distortion increased and the plastic deformation became visible. the stent was at the plastic instability stage. In this scenario, the stent's radial distortion became more noticeable.

The stents A1, B1, C1, D1, and E1 with the lowest diameter of 12 mm and other similar geometric parameters showed the largest radial force and the best resistance against compressive distortion among each group of PLA stents (A, B, C, D, and E). The experimentation clearly shows that the 3D-printed PLA auxetic stent has a similar structural thickness and that the dimensional specifications of auxetic structures had a better resistance to compressive distortion as the stent diameter reduced, as well as a stronger radial force. The three 3D-printed stents in groups A, B, and C all have the same geometrical specifications but distinct strut thicknesses. Observation shows that the C1 (Fig. 9A) having the lowest stent diameter and highest stent thickness is showing maximum resistance force as compared to other sets refer to Fig. 10. This concluded that the lowest stent diameter and highest stent thickness give the maximum radial strength keeping the other geometrical parameters the same.

The response curve has noticed few discontinuities. This phenomenon can be easily explained with an understanding of the mechanism of fused deposition modeling. The appearance of these discontinuities is due to the local fracture of the supporting strut part of the stent during the compression test. In FDM 3D printer creates the stratified effect on the surface of the printed part refer to Fig. 11. This is visualized as the staircase effect or ladder-like phenomenon. This is caused by the different boundaries of the adjacent layer when sliced layers are stacked on each other creating the irregularities on the final surface[33,34].

b) **When the stent strut Thickness is the same (considering Group B, D, and E)**

The stents in the B, D, and E groups have the same 1.5 mm strut diameter, but their auxetic structure's geometric properties vary. The group of stents (B, D, and E) with the same diameter but differing geometrical characteristics were compared for their radial compressive qualities. Figure 12 displays the radial force vs. radial displacement for groups B, D, and E. E has the greatest radial force among the designated groups, followed by the D group and B group. When

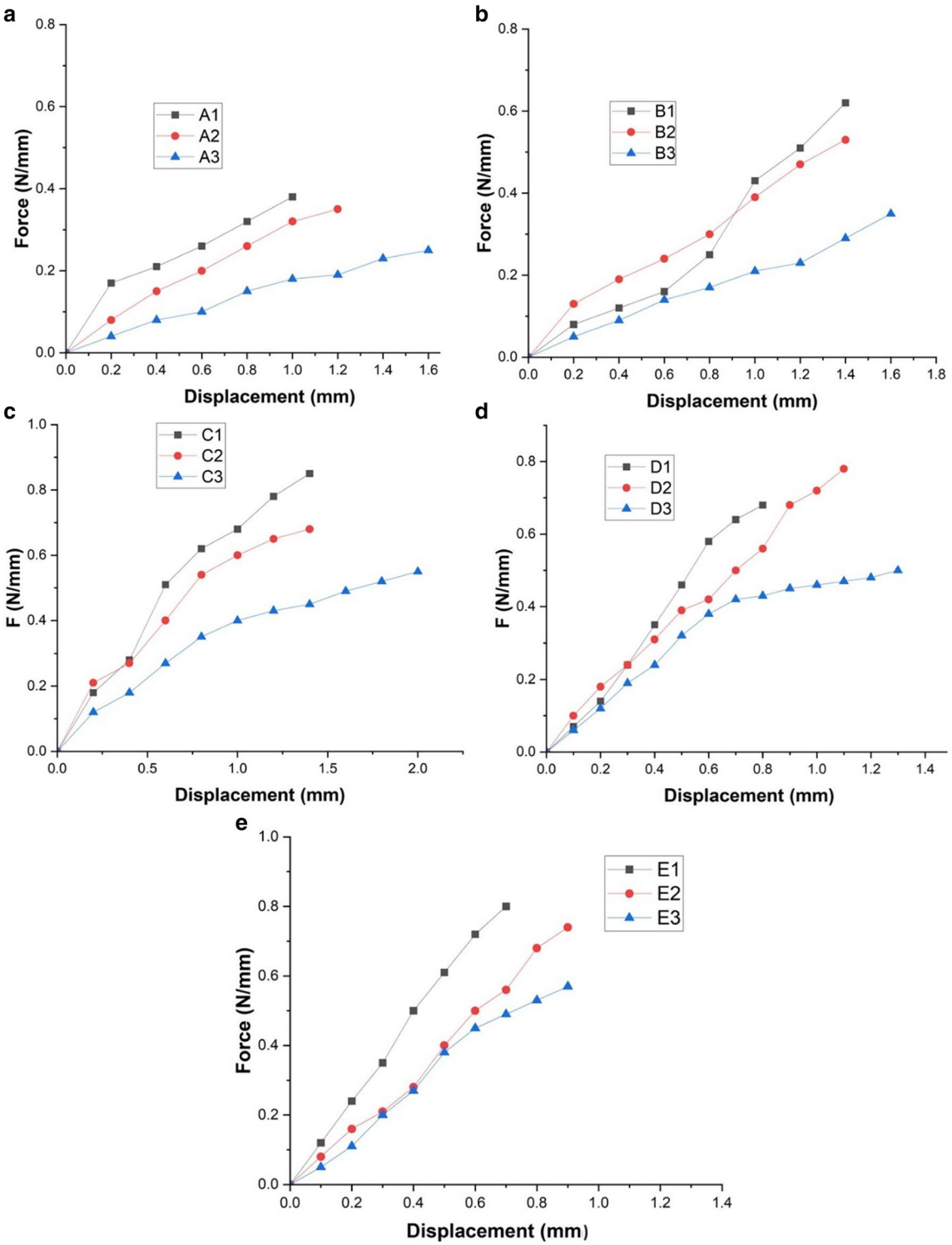

Fig. 8 For various groups (**a**, **b**, **c**, **d**, and **e**) of 3D printed PLA vascular stents, the radial force per unit length versus radial displacement curve is shown

the stent diameter remained the same, the lengths L, m, and h became small due to the rise in angle ϕ and θ, increasing the stent's surface coverage. More surface coverage resulted from the maximum value of $\phi = 30^0$ and $\theta = 65^0$, on the set of stents E1, resulting in higher compressive properties and additional material being deformed to resist distortion under the same compressive stress shown in the Fig. 12 by a red-colored circle.

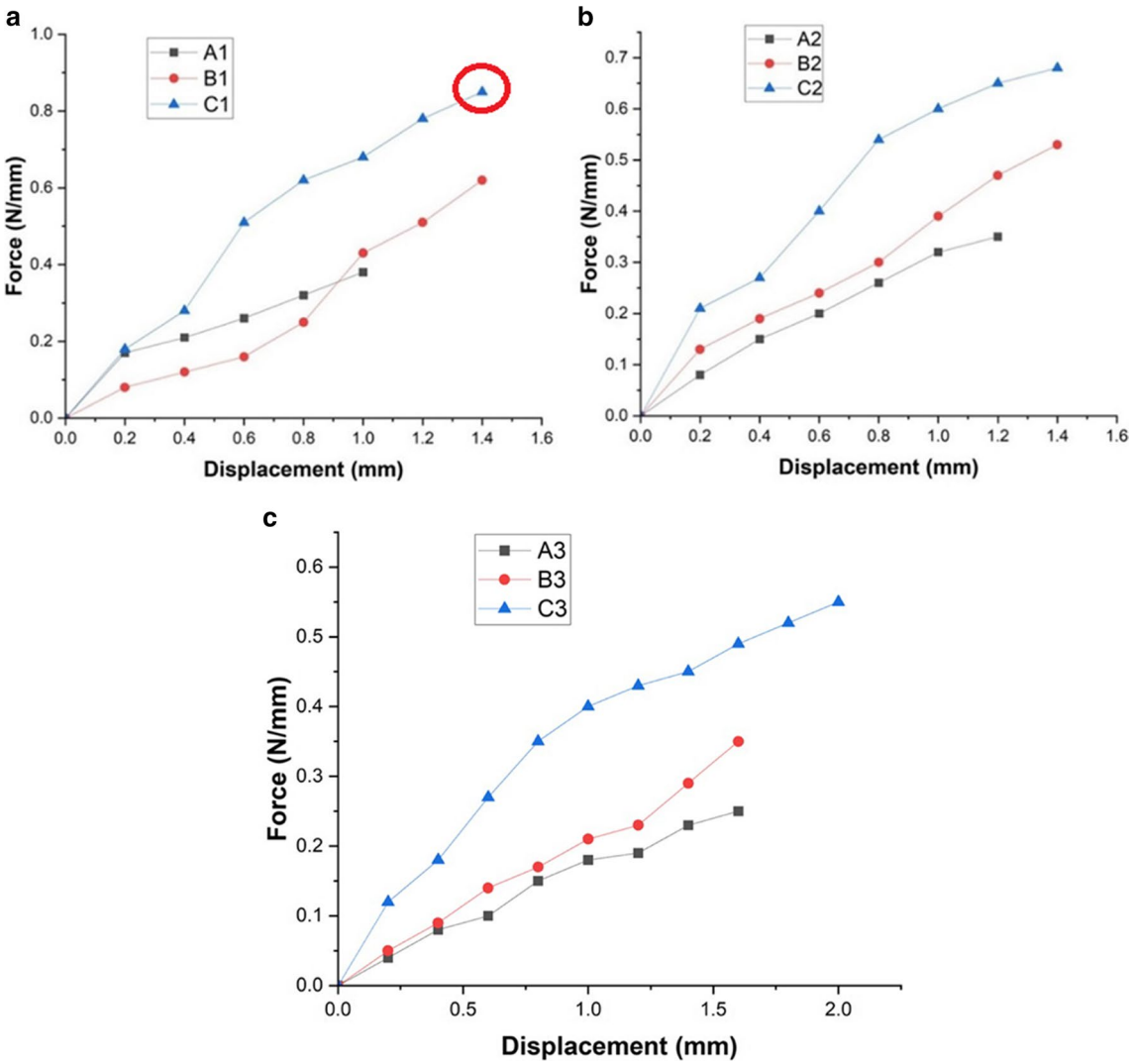

Fig. 9 Radial force per unit length (N/mm) versus radial displacement (mm) curves for different wall thicknesses of 3D-printed PLA stents (**a**) PLA vascular stents with 12 mm stent diameter; (**b**) PLA vascular stents with 14 mm stent diameter. (**c**) PLA vascular stents with 16 mm stent diameter

3.2 Shape memory experiment result of PLA Stent: (Experiment in the radial direction)

The perceived initial length and diameter Di at room temperature, the following measurements were made: the recovery diameter Dr and length Hc, the crimped diameter Dc and length Hc (Table 4). The diameter recovery ratio and length recovery ratio were calculated.

The experimental results show that the crimped length Hc, and diameter Dc are smaller than the original length & diameter (Hi and Di). This suggests that the temperature-induced deformation of the 3D-printed double arrowhead PLA stent caused it to crimp. Furthermore, it has been noted that the diameter and length recovery measures (Dr and Hr) were larger than the crimped measurements (Dc & Hc) of diameter and length. The capacity of the double arrowhead 3D printed PLA stent to concurrently contract in width and length made it possible for it to be inserted with minimal discomfort and to be transported to the deposited plague site with ease. The PLA stent's increased radial and longitudinal dimensions would prevent foreshortening and enable strong adherence to artery walls.

The SME experimental results show that Arrowhead 3D printed stent has appreciative Shape memory properties. The value for the Radial Recovery ratio for each stent is above 91% and even up to 95% when the recovery temperature and deformation temperature were both 60 ^{0}C. When the RH exceeded 97%, it essentially returned to its previous form.

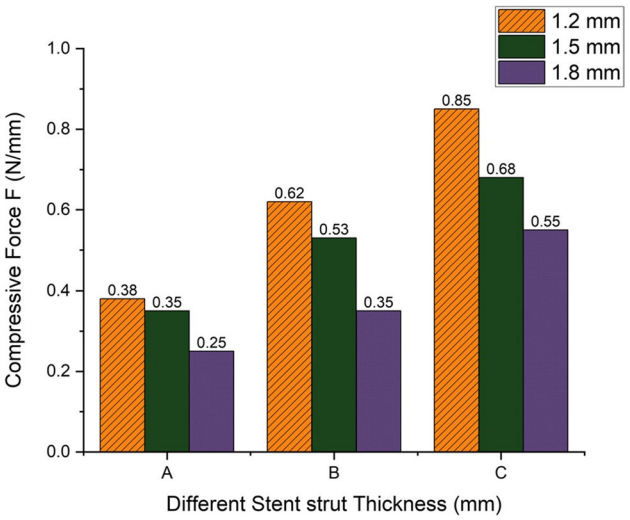

Fig. 10 Compressive strength for different stents with different strut thicknesses. (**A**: 1.2 mm, **B**: 1.5 mm, **C**: 1.8 mm)

However, other structural parameters such as the diameter of the strut and length of the strut have no obvious effect on the Shape memory effect on 3D printed Auxetic structured stent.

4 Discussion

The mechanical performance of polymeric stents made with additive manufacturing can be enhanced by optimizing the design and manufacturing parameters. Three primary factors determine the stent's strength and flexibility: strut thickness, stent pattern, and material. Adequate radial strength is necessary to sustain the lumen opening and endure the dynamic loading brought on by the blood pressure while performing the scaffolding function on the impacted area. Thus, a good stent should have minimal rebound, elevated radial strength for scaffolding, and great flexibility to facilitate smooth delivery. In the present study based on the understanding of the distortion behavior of the PLA specimen, Investigations were conducted on PLA cylindrical stents' general mechanical attributes, such as their radial strength, expanding, and crimping behaviors. The study focuses on the significance of the stent geometric design and its mechanical properties. From this analysis, we achieved the lowest stent diameter and the highest strut thickness among the set of diameters, and the strut thickness setting gives the highest radial strength required for the polymeric stent. The majority of stents used in clinical practice today are made up of metallic materials that are not biodegradable. In the efforts to develop the polymeric bioabsorbable stent made up of PLA, the current study proposes a specimen to make use of the existing stent design which gives the flexibility to increase the radial strength and shape memory effect by altering the crucial parameters during the 3D printing of the stent. One of the constraints of this research work is the neglecting the frictional effect during the expansion and crimping of the stent in the shape memory experimentation which may cause a deviation in the actual reading of the crimped dimensions. Nevertheless, the results from the shape memory experiment were quantitively analyzed, and the results were measured in terms of diametral and length recovery ratio. According to the findings of experiments performed, It was feasible to use the exciting feature shape memory effect of PLA to understand the self-extension behavior under temperature excitement above the body temperature for a PLA stent. The temperature used for PLA form memory recovery was maintained at roughly 60^0 C, which is typically greater than body temperature. It has also been noted that altering the material and using other techniques might change the recovery temperature. The shape memory experiment with 3D-printed PLA Auxetic structure stents reveals once again how excellently technology can be applied in the biomedical field. The temperature-induced deformation makes it appropriate for delicate applications like stents, where the geometric

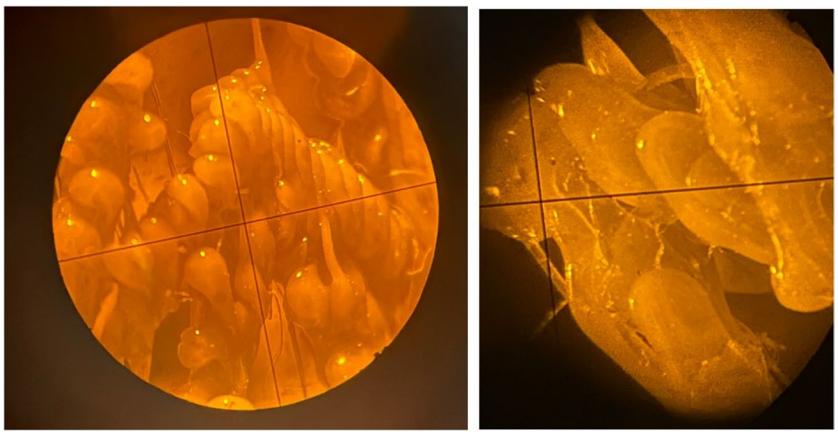

Fig. 11 Optical Microscopic view of PLA stent surface (showing deposition layers)

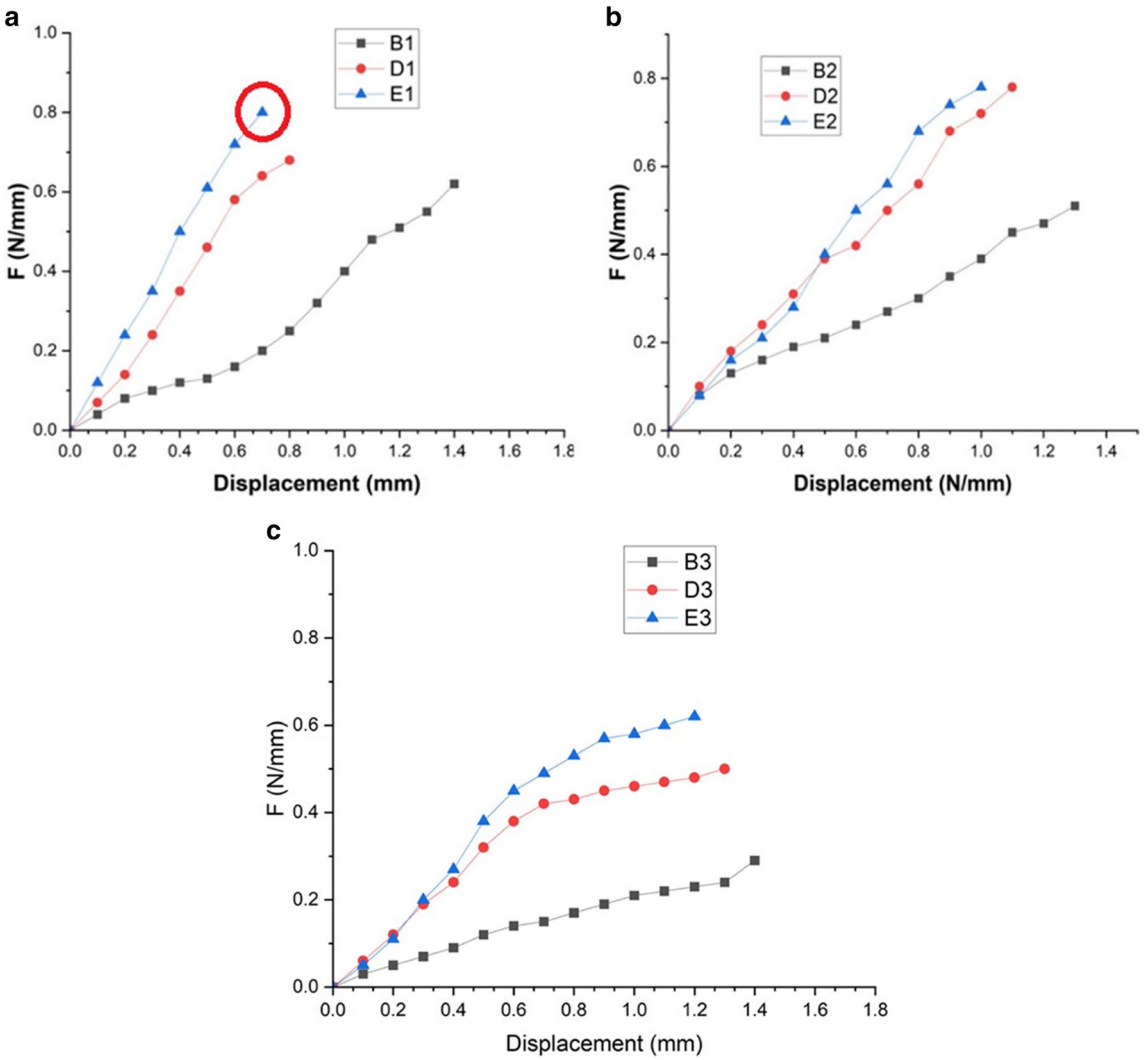

Fig. 12 For the groups B, D, and E of 3D printed PLA vascular stents, the radial force per unit length versus radial displacement curve is shown

specifications of PLA stents with an arrowhead shape were employed.

5 Conclusion

This research presents the creation of arrowhead PLA stent constructions using fused filament deposition mechanism-based additive manufacturing. Through a compression experiment, the impact of the strut diameter, stent diameter, and arrowhead structure factors on the radial compressive strength of the 3D-printed stent was investigated. Two perspectives were used to analyze the radial strength: the longitudinal and the axial directions. The influence of the stent and the strut diameter of the polymeric stent on stent mechanical performance is summarized based on experimental results:

1. The lowest stent diameter gives maximum radial strength keeping other geometrical parameters the same. The stents in each group (A, B, C, D, and E) with the lowest diameter of 12 mm showed the best resistance to compressive deformation and the maximum radial force.
2. It is apparent that when strut diameter increases the support cross-section resulting from the maximum value of θ and ϕ total coverage area increases, increasing the compression strength of the stent. The increased values of θ and ϕ take the leverage of auxetic structured double arrowhead stent. Specifically, the maximum values of stent strut thickness in all sets of testing, which was

Table 4 Results of SME experiment for 3D printed PLA stent

Group	Number	D_i (mm)	H_i (mm)	D_c (mm)	H_c (mm)	D_r (mm)	H_r (mm)	R_D	R_H
A	A1	12.20	39.84	10.25	38.54	11.35	38.02	0.9303	0.9543
	A2	14.24	39.06	12.30	37.21	13.20	38.15	0.9269	0.9767
	A3	16.14	39.65	14.65	37.68	15.25	38.62	0.9448	0.9740
B	B1	12.09	39.57	10.86	38.10	11.35	39.10	0.9387	0.9881
	B2	14.21	40.10	13.12	38.54	12.88	39.13	0.9064	0.9758
	B3	16.35	39.98	14.12	37.87	15.32	38.54	0.9370	0.9639
C	C1	12.22	39.68	10.28	37.93	11.45	38.21	0.9369	0.9629
	C2	14.34	39.80	12.41	37.56	13.66	38.05	0.9525	0.9560
	C3	16.21	39.54	14.06	37.63	15.52	38.57	0.9574	0.9754
D	D1	12.03	41.52	10.67	39.65	11.48	40.32	0.9542	0.9710
	D2	14.51	41.63	12.48	39.20	13.60	38.96	0.9372	0.9358
	D3	16.25	42.01	15.15	39.45	14.82	38.74	0.9120	0.9221
E	E1	12.63	41.25	10.65	40.30	11.74	40.14	0.9295	0.9730
	E2	14.20	41.48	12.39	39.10	13.35	38.20	0.9401	0.9209
	E3	16.61	41.21	14.68	39.66	15.41	38.52	0.9277	0.9347

1.8 mm, were shown to have the highest radial force. The stent's surface covering area varies in response to modifications in the other geometric parameters (listed in Table 3).

The diameter and length variations of the PLA stents were measured both before and after the SME experiment. Measurements were made of the length recovery ratio and diameter recovery ratio.

The SME experiment demonstrates how the 3D-printed arrowhead stent shrinks and grows at the same time in terms of both length and diameter. At 60^0 C, which is the deformation and recovery temperature, the diameter recovery ratio and the length recovery ratio were recorded at 95% and 98%, respectively. It has been established that it is possible to exploit PLA's shape memory function to revert to its original shape when exposed to temperature fluctuations, even if PLA's glass transition temperature is greater than the normal human body temperature. Because PLA has a form memory ability that allows it to return to its previous shape when exposed to temperature changes, it is therefore advised to employ this shape. Additionally, the stent's arrowhead form will strengthen its anchoring in the artery.

6 Future Scope of the Work

In the future, further efforts will be given to improve the surface roughness and dimensions of the same designed PLA stent created from 3D printing.

7 Author(s) contribution

In the paper " Proof of concept study for radial compression strength & Shape memory effect of 3D Printed Double arrowhead PLA Stent" the author(s) made the following contributions: Research Scholar Ayushi Thakur works at Amity University Uttar Pradesh in Noida, India. She is working toward a mechanical engineering doctorate. With the help of Dr. Umesh Kumar Vates, an associate professor in the mechanical engineering department at Amity University in Uttar Pradesh, India, she drew out, constructed, and produced the specimen using a 3D printer. He received his Ph.D. in Mechanical Engineering from the Institute of Technology Dhanbad, a nationally significant institution. He oversees and encourages the aforementioned PhD researcher in his capacity as an expert in this field. In this research project, he has recommended using an experimental method. At Gorakhpur, India's Madan Mohan Malviya University of Technology, Dr. Sanjay Mishra teaches as an associate professor. He has interpreted the experimental data and inspired the aforementioned PhD student.

Acknowledgements Acknowledged are the research facilities and assistance provided by ITS College of Engineering & Technology, Greater Noida, India, and Amity University, Noida, India. Samples were manufactured on-site at Creality Ender (3D Printer). The authors also thank the editors and peer reviewers for their insightful recommendations.

Funding The was no external funding was received to conduct the research.

Data availability Not Applicable.

Declarations

Conflict of Interests No potential conflicts of interest were disclosed by the author(s) regarding the research, writing, or publication of this paper.

References

1. Wei, Yunbo, et al. "Structural design of mechanical property for biodegradable polymeric stent." Adv. Mater. Sci. Eng. 2019: 1–14 (2019). https://doi.org/10.1155/2019/2960435
2. Tingzhang Hu et al., Biodegradable stents for coronary artery disease treatment: Recent advances and future perspectives. Mater. Sci. Eng.: C **91**, 163–178 (2018). https://doi.org/10.1016/j.msec.2018.04.100
3. H. Tan, R. Ananthakrishna, A review of bioresorbable scaffolds: hype or hope? Singapore Med. J. **58**(9), 512–515 (2017). https://doi.org/10.11622/smedj.2016178
4. J.-M. Ahn, D.-W. Park, S.J. Hong et al., Bioresorbable vascular scaffold Korean expert panel report. Korean Circulation J. **47**(6), 795–810 (2017). https://doi.org/10.4070/kcj.2017.0300
5. S. Borhani, S. Hassanajili, S.H. Ahmadi Tafti, S. Rabbani, Cardiovascular stents: overview, evolution, and next generation. Progress in Biomaterials **7**(3), 175–205 (2018). https://doi.org/10.1007/s40204-018-0097-y
6. J.S. Soares Jr., J.E. Moore, Biomechanical challenges to polymeric biodegradable stents. Ann. Biomed. Eng. **44**(2), 560–579 (2016). https://doi.org/10.1007/s10439-015-1477-2
7. S.H. Im, Y. Jung, S.H. Kim, Current status and future direction of biodegradable metallic and polymeric vascular scaffolds for next-generation stents. Acta Biomaterial **60**, 3–22 (2017)
8. Iwona Rykowska, Iwona Nowak, R. Nowak, Drug-eluting stents and balloons—materials, structure designs, and coating techniques: a review. Molecules **25.20**, 4624 (2020)
9. J.P. Hytonen, J. Taavitsainen, S. Tarvainen, SYl.Ä. Herttuala, Biodegradable coronary scaffolds: their future and clinical and technological challenges. Cardiovascular Research **114**(8), 1063–1072 (2018)
10 T.R. Welch, A.W. Nugent, S.R. Veeram Reddy, Biodegradable stents for congenital heart disease. Interventional Cardiology Clinics **8**(1), 81–94 (2019)
11. D. Lindholm, S. James, Bioresorbable stents in PCI. Curr. Cardiol. Rep. **18**(8), 1–6 (2016)
12. T. Li, F. Liu, L. Wang, Enhancing indentation and impact resistance in auxetic composite materials. Compos. B Eng. **198**, 108229 (2020)
13. Swetha, T. Angelin, et al. "A comprehensive review on polylactic acid (PLA)–Synthesis, processing, and application in food packaging." Int. J. Biological Macromolecules 123715 (2023) https://doi.org/10.1016/j.ijbiomac.2023.123715
14 Priya Bansal et al., Applications of some biopolymeric materials as medical implants: An overview. Materials Today: Proceedings **65**, 3377–3381 (2022)
15. A. Przybytek et al., Preparation and characterization of biodegradable and compostable PLA/TPS/ESO compositions. Ind. Crops Prod. **122**, 375–383 (2018). https://doi.org/10.1016/j.indcrop.2018.06.016
16. S. Yang, Y. He, J. Leng, Shape memory poly (ether ether ketone) s with tunable chain stiffness, mechanical strength and high transition temperatures. Int. J. Smart Nano Mater. **13**(1), 1–16 (2022)
17 Sabrina M. Curtis et al., TiNiHf/SiO2/Si shape memory film composites for bi-directional micro actuation. Int. J. Smart Nano Mater. **13.2**, 293–314 (2022)
18 Hamid Ikram, Ans Al Rashid, Muammer Koç, Additive manufacturing of smart polymeric composites: Literature review and future perspectives. Polymer Composites **43.9**, 6355–6380 (2022)
19 Farnoosh Ebrahimi, Hossein Ramezani Dana, Poly lactic acid (PLA) polymers: from properties to biomedical applications. Int. J. Polymeric Mater. Polymeric Biomaterials **71.15**, 1117–1130 (2022). https://doi.org/10.1080/00914037.2021.1944140
20 Hao Duan et al., A thermoviscoelastic finite deformation constitutive model based on dual relaxation mechanisms for amorphous shape memory polymers. Int. J. Smart Nano Mater. **14.2**, 243–264 (2023)
21. Z. Lyu, J. Wang, Y. Chen, 4D printing: interdisciplinary integration of smart materials, structural design, and new functionality. Int. J. Extreme Manufacturing **5**(3), 032011 (2023)
22. Cheng Lin et al., Mass-producible near-body temperature-triggered 4D printed shape memory biocomposites and their application in biomimetic intestinal stents. Composites Part B: Eng. **256**, 110623 (2023)
23. C. Lin, L. Zhang, Y. Liu et al., 4D printing of personalized shape memory polymer vascular stents with negative Poisson's ratio structure: A preliminary study. Sci. China Technol. Sci. **63**, 578–588 (2020). https://doi.org/10.1007/s11431-019-1468-2
24. Zichao Wu et al., Radial compressive property and the proof-of-concept study for realizing self-expansion of 3D printing polylactic acid vascular stents with negative Poisson's ratio structure. Materials **11.8**, 1357 (2018). https://doi.org/10.3390/ma11081357
25. A.M. Sousa, A.M. Amaro, A.P. Piedade, Structural design optimization through finite element analysis of additive manufactured bioresorbable polymeric stents. Materials Today Chemistry **36**, 101972 (2024)
26. M. Abbaslou, R. Hashemi, E. Etemadi, Novel hybrid 3D-printed auxetic vascular stent based on re-entrant and meta-trichiral unit cells: finite element simulation with experimental verifications. Materials Today Communications **35**, 105742 (2023)
27. Roxanne Khalaj et al., 3D printing advances in the development of stents. Int. J. Pharmaceutics **609**, 121153 (2021)
28 Huipeng Xue et al., Design of self-expanding auxetic stents using topology optimization. Front. Bioeng. Biotechnol. **8**, 736 (2020)
29 Sukhwinder K. Bhullar et al., Characterizing the mechanical performance of a bare-metal stent with an auxetic cell geometry. Appl. Sci. **12.2**, 910 (2022). https://doi.org/10.3390/app12020910
30. R.G. Pauck, B.D. Reddy, Computational analysis of the radial mechanical performance of PLLA coronary artery stents. Med. Eng. Phys. **37**(1), 7–12 (2015). https://doi.org/10.1016/j.medengphy.2014.09.014
31 Zhengkai Zhang et al., Application of double arrowhead auxetic honeycomb structure in displacement measurement. Sensors and Actuators A: Physical **333**, 113218 (2022). https://doi.org/10.1016/j.sna.2021.113218
32. A. Thakur, U.K. Vates, S. Mishra, Parametric optimization of 3D-printed PLA part using response surface methodology for mechanical properties. Smart Science (2023). https://doi.org/10.1080/23080477.2023.2270819